

Room temperature nonlinear transport in ballistic nanodevices

T González, B G Vasallo, D Pardo and J Mateos

Departamento de Física Aplicada, Universidad de Salamanca, Plaza de la Merced s/n, 37008 Salamanca, Spain

Received 28 July 2003

Published 3 March 2004

Online at stacks.iop.org/SST/19/S125 (DOI: 10.1088/0268-1242/19/4/044)

Abstract

We present a Monte Carlo analysis of InAlAs/InGaAs-based four-terminal ballistic rectifiers operating at room temperature. The rectifying effect is explained in terms of the vertical asymmetry of electron concentration originating, in the presence of ballistic transport, from the action of the obstacle located at the centre of the structure. An increase in temperature is found to degrade the performance of the structures as transport becomes more diffusive. Different geometries of the rectifier are analysed.

1. Introduction

Several GaAs/AlGaAs and InP/InGaAs nanodevices with principles of operation based on the presence of electron ballistic transport have been demonstrated in recent years, such as T- [1] and Y-branch junctions [2, 3] (TBJs and YBJs, respectively) or ballistic rectifiers [4, 5]. Some of them are able to work at room temperature thanks to the long mean-free-path of electrons in InGaAs, still larger than 100 nm at $T = 300$ K [5]. These devices are promising candidates for data-processing applications at ultra-high bit rate (even in the THz frequency range).

Theoretical models for the operation of these ballistic devices have been proposed in the literature [6–8], typically based on a coherent transport description. However, phase coherence, which is normally lost at room temperature, is not essential for modelling the measured ballistic effects. As an alternative, in this work we use a semiclassical Monte Carlo (MC) simulator for the analysis of these devices. The experimental measurements reported in the literature for the nonlinear ballistic effects taking place in these structures are qualitatively reproduced and thoroughly explained by our model [9, 10], taking as a base the presence of space charge, which appears mainly due to the surface charge located at the semiconductor–air interfaces and the action of the injecting contacts [11]. As a prototype to show the capability of MC simulations to deal with these ballistic nanodevices, here we will focus our analysis on an InAlAs/InGaAs-based four-terminal ballistic rectifier, originally proposed by Song *et al* [4]. The versatility of the MC method allows us to analyse the temperature behaviour of the rectifier and the influence of different possible geometries.

2. Physical model

The device under analysis is made by inserting a scatterer (antidot), typically triangular, at the centre of a ballistic cross junction, as shown in the inset of figure 1 (where the dimensions of the structure are also indicated). For the calculations we use a semiclassical ensemble MC simulator, which includes all the details of scattering mechanisms, self-consistently coupled with a two-dimensional (2D) Poisson solver. Since contact injection is a critical point when dealing with ballistic transport, the velocity distribution and time statistics of injected carriers at the left and right branches are accurately modelled following [11, 12]. Top and bottom branches remain open circuited. For exact analysis of these devices, a three-dimensional (3D) simulation would be necessary to take into account the effect of the lateral surface charges and the real layer structure. When using the 2D MC model, some simplifications must be made. We perform a top-view simulation of the device, where the real layer structure is not included, and only the InGaAs channel is simulated. In order to account for the fixed positive charges of the whole layer structure, a net doping is assigned to the channel, but impurity scattering is switched off. On the other hand, a negative surface charge density is assigned to the semiconductor–air interfaces to account for the influence of the surface states originated by the etching processes. Therefore, the values of three important parameters must be carefully chosen: the *effective* doping of the injecting contacts, N_C , the background doping in the channel, N_{Db} , and the lateral surface charge density, σ . We will consider $N_C = 4 \times 10^{17} \text{ cm}^{-3}$ and $N_{Db} = 10^{17} \text{ cm}^{-3}$ values for which a reasonable agreement with experiments in ballistic channels has been found [9]. More details about the model can be found in [10].

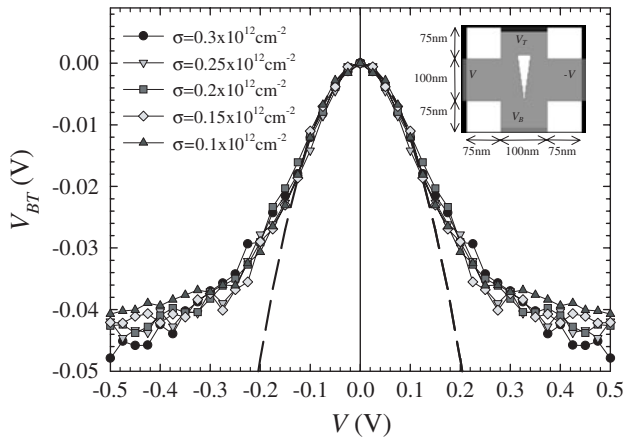


Figure 1. Potential difference between bottom and top branches, V_{BT} , as a function of V when biasing with $V = V_L = -V_R$ the left and right branches of the ballistic rectifier with the geometry shown in the inset, for several values of lateral surface charge σ . $T = 300$ K. The dashed line is a parabolic fitting of the results for low values of V .

3. Results

Figure 1 shows the values of the potential difference between the bottom and top branches, $V_{BT} = V_B - V_T$, obtained from the MC simulation of the ballistic rectifier sketched in the inset at room temperature when biasing left and right branches in push-pull fashion, $V = V_L = -V_R$, for several values of the lateral surface charge σ . The behaviour found in the simulations is in excellent qualitative agreement with experimental findings [5]. As in TBJs or YBJs [1–3], when biasing right and left branches with $V = V_L = -V_R$, a negative potential always appears in the central branch, which increases with V [10]. In the case of the rectifier, the negative potential is generated in both central branches (bottom and top), but with different values due to the unequal width of the opening space between the horizontal and the top/bottom branches, which leads to an asymmetric injection of carriers into them. The narrower the space between the horizontal and vertical branches, the higher the potential barrier created by the lateral surface charge and the lower the probability of an electron to pass from one branch to the other. This can be clearly observed in the 2D chart of electron concentration shown in figure 2. The stronger injection of carriers into the bottom branch (because of the asymmetric geometry of the obstacle) enhances the curvature of the V_B values versus V when compared to that of V_T . As a consequence, negative values are obtained for V_{BT} , which depend mainly on the size and shape of both the obstacle and the different branches. Remarkably, even if the values of both V_B and V_T are found to depend on σ , their difference V_{BT} is almost constant, as observed in figure 1. This happens because the different curvature of V_B with respect to V_T comes from the unequal penetration of carriers into the top and bottom branches, and this difference remains nearly unchanged with σ in the range of σ values reported in the figure. The efficiency of this ballistic rectifier reaches 15% at $V = 0.2$ V, in good agreement with the experimental results shown in [5]. The origin of the rectifying behaviour of this device can therefore be understood as a consequence of (i) the

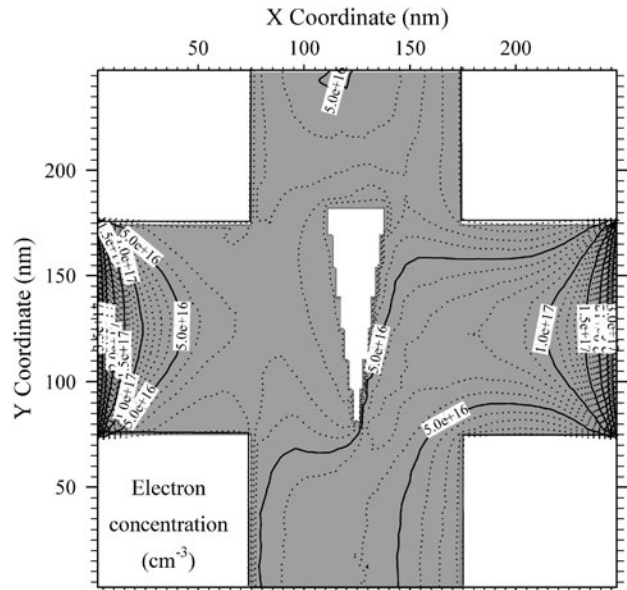


Figure 2. 2D contour plot of electron concentration in the ballistic rectifier of figure 1 for $V = V_L = -V_R = 0.2$ V and $\sigma = 0.25 \times 10^{12} \text{ cm}^{-3}$.

horizontal asymmetry of the electron concentration associated with both ballistic transport and space charge inside the device, and (ii) the different openings between the horizontal and top/bottom branches (or, following the formalism of [6], the different transmission coefficients between them). These two factors originate the observed vertical asymmetry of electron concentration, and thus of electric potential. As in the case of TBJs and YBJs, the behaviour of V_B and V_T (and thus of V_{BT}) for low V remains parabolic up to a given biasing, for which the unbalanced injection of charge into the top and bottom branches reaches a saturation regime and V_{BT} takes a constant value. The intrinsic capability of this device for rectification at extremely high frequencies has been checked by analysing the V_{BT} response to periodic AC signals applied between left and right electrodes. An excellent performance as a frequency doubler or power detector in the THz range (at least up to 1 THz) has been found [10].

Figure 3 shows the temperature dependence of the rectifying behaviour of the structure. When the temperature is raised above 300 K, the rectifying effect is less pronounced (lower absolute values of V_{BT}), as expected from the increasing influence of scattering mechanisms. Transport in the structure approaches the diffusive regime, thus reducing the influence of the asymmetric shape of the scatterer on the injection of carriers into the top/bottom branches. In the case of purely diffusive transport the effect should disappear, since carriers would be equally injected by diffusion into both central branches. In contrast, for the lowest temperatures (77 and 150 K), the rectifying effect is enhanced (higher absolute values of V_{BT}), reaching an efficiency of 20% at $V = 0.2$ V. The results are very similar for 77 and 150 K, thus indicating that in both cases transport is practically ballistic. Note that for 300 K, even if the effect is important, transport is still quasi-ballistic.

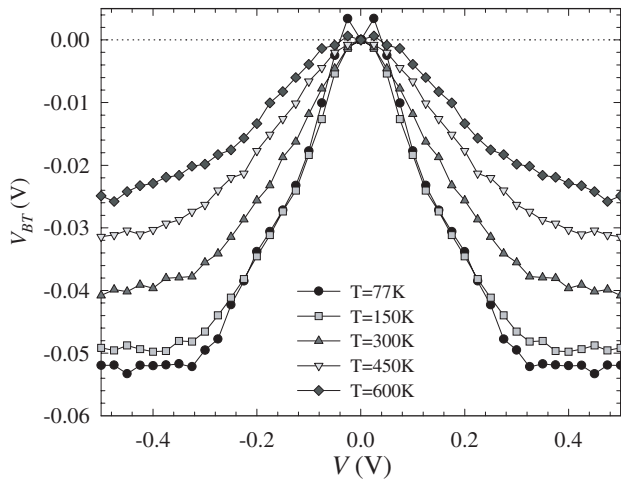


Figure 3. V_{BT} versus $V = V_L = -V_R$ for several temperatures in the ballistic rectifier of figure 1 with $\sigma = 0.25 \times 10^{12} \text{ cm}^{-3}$.

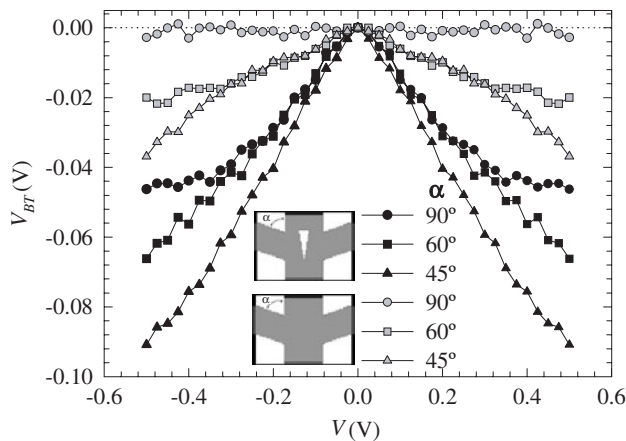


Figure 4. V_{BT} versus $V = V_L = -V_R$ in the ballistic rectifiers sketched in the insets at $T = 300 \text{ K}$ for several opening angles α of the lateral branches. Closed (open) symbols correspond to structures with (without) a central scatterer. $\sigma = 0.25 \times 10^{12} \text{ cm}^{-3}$.

The influence of the geometry of the device on the rectifying effect is illustrated in figure 4, where we show results for structures with and without a central scatterer, and for different opening angles α of the lateral branches with respect to the top branch. As expected, the absence of a scatterer leads to the complete disappearance of the effect for the case of $\alpha = 90^\circ$, due to the vertical symmetry of the structure. However, even in the absence of a scatterer, opening angles lower than 90° lead to the appearance of negative values of V_{BT} (of higher magnitude for smaller α) due to the asymmetric injection of carriers into the top/bottom branches assisted by the opening angle and

the quasi-ballistic character of transport in the structures. In the presence of a scatterer, values of α below 60° lead to an important enhancement of the rectifying effect by intensifying the injection of carriers into the bottom branch. For $\alpha = 45^\circ$, an efficiency of 20% is obtained at $V = 0.2 \text{ V}$. Interestingly, the saturation regime in V_{BT} is displaced to higher values of V as α is decreased.

4. Conclusions

The asymmetric injection of carriers into the vertical branches of a four-terminal ballistic cross junction originating from the presence of an obstacle in the centre of the structure has been found to be responsible (assisted by electron ballistic transport) for the rectifying behaviour of the device. The effect can be enhanced by appropriately orienting the lateral branches. The quasi-ballistic character of transport in these structures allows them to perform at room temperature up to extremely high frequencies, even reaching the THz range.

Acknowledgments

This work has been partially supported by the European Commission through the NANOTERA project IST-2001-32517, by the Dirección General de Investigación (Ministerio de Ciencia y Tecnología) and FEDER through the project TIC2001-1754 and by the Consejería de Cultura de la Junta de Castilla y León through the project SA057/02.

References

- [1] Shorubalko I, Xu H Q, Maximov I, Omling P, Samuelson L and Seifert W 2001 *Appl. Phys. Lett.* **79** 1384
- [2] Hieke K and Ulfward M 2000 *Phys. Rev. B* **62** 16727
- [3] Worschech L, Xu H Q, Forchel A and Samuelson L 2001 *Appl. Phys. Lett.* **79** 3287
- [4] Song A M, Lorke A, Kriele A, Kothaus J P, Wegscheider A and Bichler M 1998 *Phys. Rev. Lett.* **80** 3831
- [5] Song A M, Omling P, Samuelson L, Seifert W, Shorubalko I and Zirath H 2001 *Japan. J. Appl. Phys.* **40** L909
- [6] Song A M 1999 *Phys. Rev. B* **59** 9806
- [7] Xu H Q 2001 *Appl. Phys. Lett.* **78** 2064
- [8] Fleischmann R and Geisel T 2002 *Phys. Rev. Lett.* **89** 016804
- [9] Mateos J, Vasallo B G, Pardo D, González T, Galloo J S, Roelens Y, Bollaert S and Cappy A 2003 *Nanotechnology* **14** 117
- [10] Mateos J, Vasallo B G, Pardo D, González T, Galloo J S, Roelens Y, Bollaert S and Cappy A 2003 *IEEE Trans. Electron. Devices* **50** 1897
- [11] González T, Bulashenko O M, Mateos J, Pardo D and Reggiani L 1997 *Phys. Rev. B* **56** 6424
- [12] González T, Mateos J, Pardo D, Varani L and Reggiani L 1999 *Semicond. Sci. Technol.* **14** L37